BCSIR

Available online at www.banglajol.info/index.php/BJSIR

Bangladesh J. Sci. Ind. Res. **60(3)**, 159-168, 2025

BANGLADESH JOURNAL OF SCIENTIFIC AND INDUSTRIAL RESEARCH

ISSN. 0304-9809

Spectral, electrical, mechanical and dielectric characterization of 2-aminobenzothiazolium 4-fluorobenzoate (Scaffold in drugs) single crystal

J. Anantha Meena Geetha[1] and S. Robinson Jebas[2]*

[1]*Research Scholar (Reg No. 21211062132002), PG and Research Department of Physics, Kamarajar Government Arts College, Surandai, Tenkasi Dt, Tamilnadu, India 627859*

[2]*Associate Professor and Head, PG and Research Department of Physics, Kamarajar Government Arts College, Surandai, Tenkasi Dt, Tamilnadu, India 627859*

[1,2] *Affiliated to Manonmaniam Sundaranar University, Abishekapatti, Tirunelveli, 627 012, Tamil Nadu, India)*

ARTICLE INFO

Received: 15 May 2025

Revised: 07 July 2025

Accepted: 14 July 2025

eISSN 2224-7157/

DOI: https://doi.org/10.3329/bjsir.v60i3.81693

Abstract

Transparent colourless block single crystal of 2-aminobenzothiazolium 4-fluorobenzoate (2-ABT4FB) was grown from aqueous solution via slow evaporation method. The unit cell parameters of the title compound was determined from single crystal x-ray diffraction studies and found to be a=12.15(9) A, b=12.65(9) A, c=28.3(2) A, α=85.03(18)˚, β=83.00(17)˚, γ=71.30(9)˚. The crystal exhibits wide transparency window of 99%. The band gap energy of the crystal was calculated as 4.11eV from the Tauc's plot. The sharp emission peak observed at the wavelength of 470 nm in the photoluminescence spectra is due to the blue emission. Mechanical stability of the grown single crystal was investigated by using Vickers microhardness test and reveals that 2-ABT4FB single crystal is the soft material with the Meyer's index (n) of 2. Single crystal exhibits high dielectric constant at lower frequencies and the dielectric loss decreases as the frequency increases is due to the various polarization effects.

Keywords: Transmittance; Urbach energy; Emission; Hardness; Dielectric constant

Introduction

Optical materials play significant role in determining the modern technologies and applications in the industry (Karuppasamy *et al.* 2020, Shubashini and Jebas, 2025). Recent years have witnessed significant advancements in optical materials within the field of science and technology, applicable to various fields including optoelectronics, optical communication, photonics, high-speed information processing, optical data storage, along with data transmission in high-energy lasers (Lee *et al.* 2016). To identify whether a material is appropriate for optoelectronic applications, it is required to study numerous crystal parameters like transmittance, absorption, extinction coefficient, reflectance, refractive index, optical conductivity, electrical conductivity as well as photoluminescence.

Benzothiazole is an important class of fused hetrocyclic scaffold having broad range of pharmaceutical applications such as antimicrobial (Al-Tel *et al.* 2011) and anticancer activities (Kamal *et al.* 2011). In material science, 2-aminobenzothiazole (2-ABT) and its derivatives have been utilized as building blocks for synthesizing functional materials, including organic semiconductors, light-emitting diodes and sensors (Ramin *et al.* 2024). The tunable electronic properties of 2-ABT make them attractive candidates for applications in optoelectronics, sensing technologies and electroluminescent devices (Frizon *et al.* 2023). The optical properties of 2-aminobenzothiazole derivatives (Jin *et al.* 2012), 2-aminobenzothiazole 2,6-pyridinedicarboxylic acid (İlkimen *et al.* 2014), N-(1,3-benzothiazole-2-yl)-2-methoxybenzamide

*Corresponding author's e-mail: jebas2@gmail.com

(Prabukanthan *et al.* 2020), aminobenzothiazole1-methylisatin (Sharma *et al.* 2020) and 2-aminobenzothiazole 5-sulfosalicylic acid (HalilIlkimen *et al.* 2018) have been reported.

4-Fluorine substitution makes fluorobenzoic acid as an important chemical in commercial applications and organic synthesis. The chemical stability and biological activity of benzoic acid can be enhanced by the addition of a fluorine atom, hence increasing their efficiency in the synthesis of agrochemicals. The scenario's significance extends across industries and research fields, contributing to the development of innovative materials, chemicals, and technologies (Hassel *et al.* 1970). The self-assembly and molecular recognition processes of crystalline materials are significantly influenced by the non-covalent interactions such as hydrogen and halogen bonding (Braga, 2007**)**. Recently, much attention has been focused on co-operation and competition between halogen and hydrogen bonds coexisting in the crystal packing of co-crystals, salts and solvates (Kornelia *et al.* 2015).

Even though 4-fluorobenzoic acid possesses excellent applications in the field of medicines, very few studies were carried out regarding the optical properties. 4-fluorobenzoic acid piperazine complex (Vijayalakshmi *et al.* 2025) and Lanthanide complexes with 4-fluorobenzoic acid (Li *et al.* 2015) have been reported.

The crystal structure of 2-aminobenzothiazolium 4-fluorobenzoate (2-ABT4FB) has been reported earlier in the literature. Aroused by the curiosity of the optical properties of 2-ABT4FB, we have grown the crystals of 2-aminobenzothiazolium 4-fluorobenzoate (2-ABT4FB) and the crystal have been characterized by Single XRD, FTIR, UV-Vis NIR, photoluminescence, mechanical and dielectric for its suitability as optical material for optoelectronic applications.

Experimental

2-aminobenzothiazole and 4-fluorobenzoic acid were purchased from Otto (India). The chemicals were used without further purification. Equimolar amounts of 2-aminobenzothiazole and 4-fluorobenzoic acid were dissolved in 25 ml ethanol separately. The clear solution of 2-aminobenzothiazole obtained was added to the solution of 4-fluorobenzoic acid in drops with continuous stirring. The mixture was stirred up for one hour with mild heating (temp 20^{o}C). The clear solution obtained was allowed to evaporate slowly by closing the mouth of the beaker with silver paper. Minute holes were made on the silver paper to pave the way for slow evaporation. Fig. 1 shows the grown crystal of 2-ABT4FB. Fig. 2 illustrates the reaction mechanism of 2-ABT4FB.

Fig. 1. Crystals of 2-ABT4FB

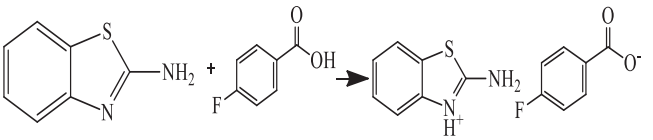

Fig. 2. Reaction mechanism of 2-ABT4FB

Results and discussion

Single XRD analysis

The unit cell parameters of the grown crystal was determined from the BRUKER Q8 QUEST Duo X-ray diffractometer. The title compound crystallizes in a triclinic crystal system with the unit cell parameters of a=12.15(9)A, b=12.65(9)A, c=28.3(2)Å , α=85.03(18)˚, β=83.00(17)Å, γ=71.30(9)Å and V= 4080.(90)Å^{3}.

Fourier transform infrared analysis

FT-IR study involves the examination of stretching, bending, twisting and vibrating modes of atoms in a molecule and hence to determine the functional groups in the crystal. Functional groups that have a strong dipole give rise to strong absorptions in the IR. Using a Perkin-Elmer Spectrometer, FTIR spectrum of the 2-ABT4FB single crystal has been recorded between 4000–400 cm^{-1} range. The protonation of hydrogen from 4-flourobenzoic acid to 2-aminobenzothiazole is confirmed by the symmetric streching of NH^{+} at 1234 cm^{-1} (Denys, 1964). The presence of amino functional group in 2-aminobenzothiazole is confirmed by the asym-

metric stretching peak at 2851 cm^{-1}. The peak at 1685 cm^{-1} indicates the C=O bond in the 4-flourobenzoate. In 2-ABT4FB, C-F out of plane deformation is observed at 1015cm^{-1} (Asep Bayu Dani Nandiyanto *et al.* 2019). The C-N bonding is the cause of the stretching band at 1314 cm^{-1} (Brain *et al.* 1989). Region 611 cm^{-1} experiences stretching vibrations attributed to C-S (Mahalakshmi and Parthasarathy 2024). Fig. 3 displays the 2-ABT4FB FT-IR spectrum.

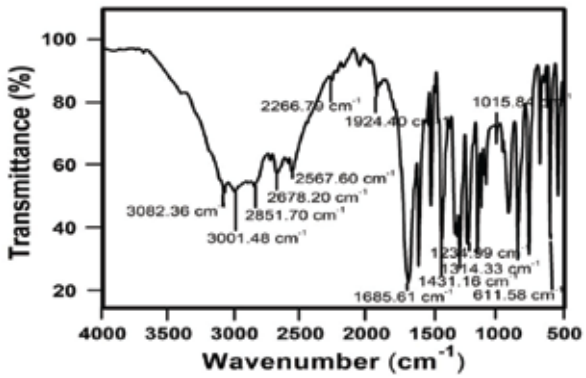

Fig. 3. FTIR spectrum of 2-ABT4FB crystal

UV-Visible spectral analysis

The 2-ABT4FB single crystal's UV-visible NIR transmittance and absorbance spectrum was recorded using the Perkin Elmer Lambda 35 Spectrophotometer, which operates in the wavelength range of 190 to 1100 nm.The trasmittance and absorbance spectra are shown in Fig. 4 and Fig. 5. The transmittance percentage of the title compound is observed to be 99%. The UV spectral analysis Fig. 4 shows that 2ABT4FB crystals have efficient relaying in the UV and Visible spectrums, which is useful for optoelectronics application. The absorption spectrum indicates that the grown 2-ABT4FB crystal having the lower cut-off wavelength at about 224 nm. The absorption peak observed at 224 nm is attributed to π-π* transitions.

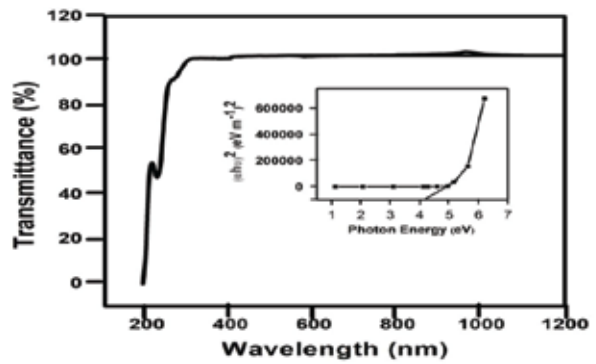

Fig. 4. Optical transmittance spectrum of 2-ABT4FB with the plot of hυ versus $(\alpha h\upsilon)^2$

Determination of band gap energy

The dependence of optical absorption coefficient on photon energy helps to study the band structure and type of transition of electrons. The optical absorption coefficient (α) was calculated from the transmittance (Mahalakshmi and Parthasarathy, 2024) using the following equation (1),

$$\alpha = \frac{2.3036 \log\left(\frac{1}{T}\right)}{d} \quad (1)$$

In this case, T stands for transmittance and d for crystal thickness. The Tauc plot method has been used to calculate the optical band gap energy (Eg) (Tauc, 1974).

$$(\alpha h\upsilon)^2 = A\,(h\upsilon - E_g) \quad (2)$$

Here, hυ stands for incident photon energy and α for optical absorption coefficient. The 2-ABT4FB crystal has band gap energy (Eg) of 4.11 eV. A graph is drawn between $(\alpha h\upsilon)^2$ versus hυ as shown in Fig. 4**.** Band gap energy of crystal conveys the capability of dielectric medium (crystal) to be polarized under the effect of strong radiation (Hiral Raval, 2019). It indicates that the crystal can be utilized as a promising material for the design of optical devices.

Determination of urbach energy

Urbach energy is the measure of defect density and trap states present in the crystal. Trapped states occur in the crystal due to the presence of impurity atoms and the thermal vibrations of lattice. Precisely speaking, the crystalline materials are exhibiting broad urbach tail at the absorption edge due to the coupling of excitons and photons (Sadat, 2014). An urbach relationship (Urbach, 1953) can be used to express the absorption coefficient in the exponential-edge region.

$$\alpha = \alpha_o \exp(h\upsilon/E_u) \quad (3)$$

Here, hυ represents incident photon energy, α represents characteristic crystal parameters, E_u represents urbach energy. Urbach energy is determined from the plot in Fig. 5, the plot which is drawn between photon energy versus absorption coefficient. The urbach energy (E_u) is determined to be 0.05eV. A lower urbach energy (E_u) value indicates smaller crystalline defects.

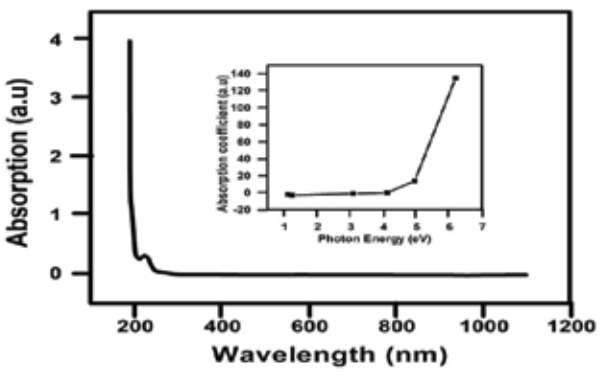

Fig. 5. Optical absorption spectrum of 2-ABT4FB ABT4FB with the plot of hυ versus α

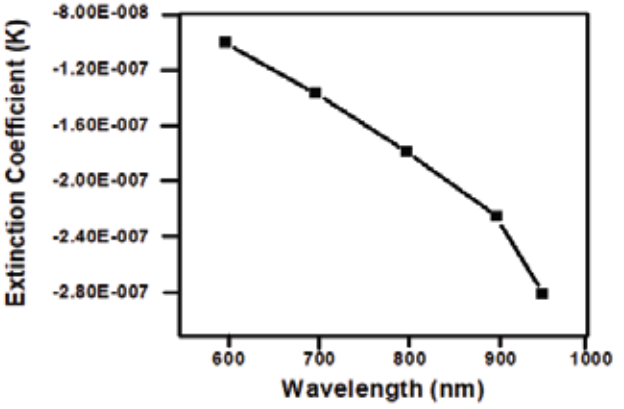

Fig. 6. Wavelength versus K

Determination of steepness parameter (σ_s) and strength of electron phonon interaction

A temperature-dependent parameter called, steepness parameter characterized by absorption edge broadening resulting from electron-phonon or exciton-phonon interactions (Mahendra *et al.* 2023). Steepness parameter has been found from the below euqation,

$$\sigma_s = \frac{K_B T}{E_u} \quad (4)$$

Here, K_B represents Boltzmann's constant 8.6173x10^{-5}eV, T represents absolute temperature and E_u represents urbach energy (0.05eV). Additionally, electron and phonon interaction strength with respect to steepness parameter given below,

$$E_{e-p} = \frac{2}{3\sigma_s} \quad (5)$$

The estimated values of steepness parameter and strength of electron-phonon interaction are 0.4707 and 1.416 eV^{-1}.

Determination of optical constant

Optical study gives information associated with the electronic band structures and compositional nature of the material (Anis *et al.* 2018). Using the following theoretical formula, various additional optical constants were determined (Dhanaraj *et al.* 2010). Extinction coefficient can be obtained from the following equation (6)

$$K = \frac{\alpha\lambda}{4\pi} \quad (6)$$

Where α is the absorption coefficient and λ is the wavelength of light. The variation of extinction coefficient with wavelength is shown in Fig.6, indicates that the extinction coefficient strongly depends upon wavelength. According to the graph, as wavelength increases, the extinction coefficient decreases. It is evident from the figure that the grown crystal exhibits a low value of extinction coefficient which indicates that there are negligible loss of light due to scattering and absorption, thus suggesting its suitability in computing devices. (Nalini *et al.* 2021, Sangeetha *et al.* 2014).

The equation (7) can be used to calculate R (reflectance) in terms of the absorption coefficient (α) and the crystal thickness (t).

$$R = 1 \pm \frac{\sqrt{1 - \exp(-\alpha t) + \exp(\alpha t)}}{1 + \exp(-\alpha t)} \quad (7)$$

Generally refractive index of a substance is the measure of the speed of light in that substance (n=c/v), is the key param-

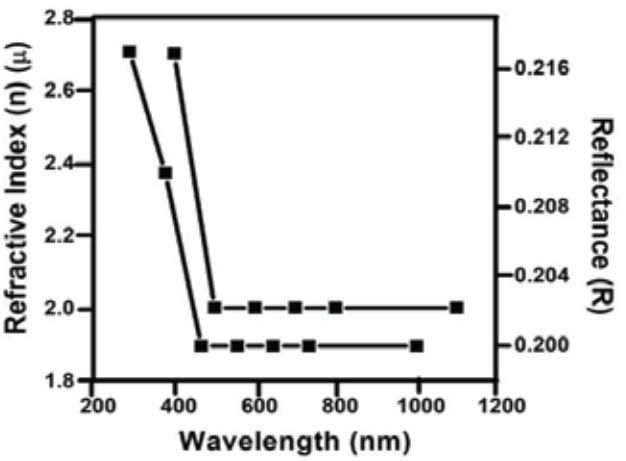

Fig. 7. Wavelength versus n versus R

eter for optical device design. The measurement of speed of refractive index n can be determined from the reflectance data using the equation (8)

$$n = \frac{-(R+1) \pm \sqrt{-3R^2 + 10R - 3}}{2(R-1)} \quad (8)$$

The calculated refractive index (n) value using the above equations for the grown 2-ABT4FB is 2.72. Fig. 7 shows the variation of the refractive index of the grown 2-ABT4FB crystal with increasing wavelength. From 280 nm to 360 nm, the refractive index of the title compound increases and then remains constant for the wavelength between 430 nm to 1000 nm. In the visible region, the magnitude of the refractive index is almost constant with a sufficiently low value. The materials having low refractive index are potential candidates in the solid-state lasers for the fabrication of optical memory storage (Tariq *et al.* 2023).

The equation (9) can be used to calculate R in terms of absorption coefficient (α) and the crystal thickness (t).

$$R = \frac{(n-1)^2}{(n+1)^2} \quad (9)$$

Graphical representation of reflectance as a function of wavelength is shown in Fig. 7. The reflectance of 2-ABT4FB crystal is calculated as R = 0.2135. From Fig.7 reflectance of the material decreases as the wavelength increases. It is the important character of the material which possesses optoelectronic properties.

Conductivity measurement

Optical conductivity is one of the important quantities that describes the optical properties of the materials. Optical conductivity is used to detect the allowed inter band optical transitions of the material (Yakuphanoglu *et al.* 2004) The optical conductivity of a material directly depends on the refractive index and absorption coefficient, and it is derived from the equation (10) (Omer *et al.* 2018),

$$\sigma_{OP} = \frac{\alpha n c}{4\pi} \quad (10)$$

The plot of optical conductivity versus wavelength is shown in Fig. 8. It is observed from the plot, in the title compound, as the wavelength increases, the optical conductivity decreases. In Fig. 9, photon energy (hϋ) is plotted against optical conductivity (σ_{op}). It illustrates how incident photon energy increases linearly with optical conductivity. The high optical conductivity of the 2-ABT4FB composition suggests perquisite features which are in high demand for designing optical information processing as well as computing devices (Anis and Muley 2016).

Electrical conductivity is the ease with which an electric charge or heat can pass through a material. The electrical conductivity is related to the optical conductivity of the crystal as (equation 11) (Murugan *et al.* 2022)

$$\sigma_e = \frac{2\lambda\sigma_{OP}}{\alpha} \quad (11)$$

Fig. 8 and Fig. 9 shows the electrical conductivity characteristics of the 2-ABT4FB single crystal. The electrical conductivity increases as the wavelength increases and the electrical conductivity decreases with respect to the photon energy. 2-ABT4FB suggesting that it is a promising material for the fabrication of electronic devices. It shows the semiconducting property of the grown crystal. From this study, the grown 2-ABT4FB crystal has inherently enhanced optical and electrical nature so, it may be used in optical as well as electrical applications.

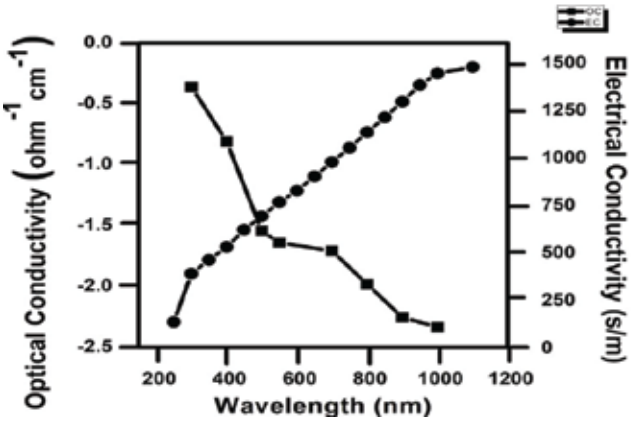

Fig. 8. Plot of λ versus σ_{op} & σ_e of 2-ABT4FB

Susceptibility is the response of medium to light (Hari Singh Nalwa, 2001). Electric susceptibility represents a quantitative measure of the extent within which an applied electric field induces polarization in a dielectric material. For calculating electric susceptibility (χ_c), the equation (13) can be used.

$$\varepsilon_r = \varepsilon_0 + 4\pi\chi_c = \eta^2 - k^2 \quad (12)$$

$$\chi_c = \eta^2 - k^2 - \varepsilon_0/4\pi \quad (13)$$

The dielectric nature of the materials is investigated using the values of the real and imaginary dielectric constants. When there is no impact from free carriers, the dielectric constant is represented by ε_o. Real and imaginary components of dielectric constant are derived from the extinction coefficient (Kochuparampil *et al.* 2017).

$$\varepsilon c = \varepsilon r + \varepsilon i \quad (14)$$

$$\varepsilon r = n^2 - k^2 \quad (15)$$

$$\varepsilon i = 2nk \quad (16)$$

Here, ε_r and ε_i are the real and imaginary components of the dielectric constants. Calculated electric susceptibility is χ_c = 0.1214, dielectric constant's ε_r and ε_i values are 1.5257 and 3.7391×10^{-6} respectively. Hence, the low magnitude of the dielectric constant with a broad energy gap of the 2-ABT4FB crystal suggests its fitness for optoelectronic devices.

Photoluminescence analysis

Light re-emission after absorbing a photon of higher energy is called photoluminescence (Mark Fox, 2013). The physical characteristics of a material, such as its purity and crystallinity, can be determined at the molecular level using photoluminescence analysis. The 2-ABT4FB single crystal was analyzed using Varian Cary Eclipse spectrophotometer. The photoluminescence spectrum was recorded in the range of 300 nm-500 nm. The emission spectrum of the 2-ABT4FB single crystal is shown in Fig. 10. The 2-ABT4FB single crystal is excited at 340 nm with an excitation energy of 3.64 eV. The broad peak observed at 470 nm (2.63) is due to blue emission. Hence the broad luminescence profile gives information about the electronic property of the grown crystal**.** The grown crystal is a material for nonlinear optical applications since it emits visible spectrum light (Yongbin *et al.* 2021).The relationship between energy (in eV) and wavelength (in nm) is given by the equation (17).

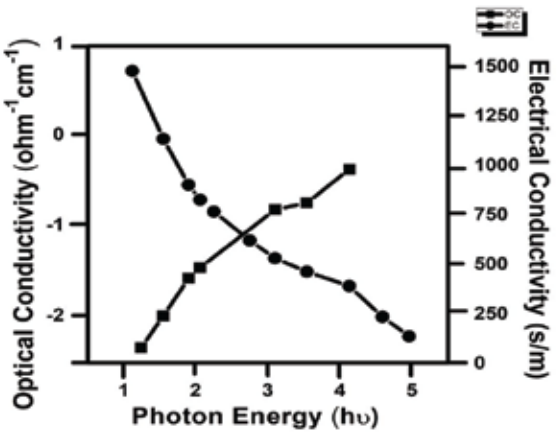

Fig. 9. Plot of Energy versus σ_{op} & σ_e of 2-ABT4FB

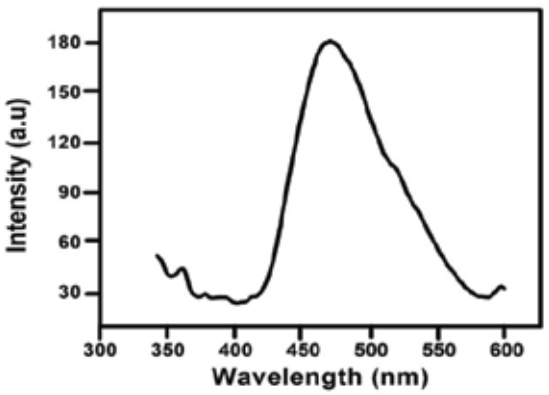

Fig. 10. Photoluminescence emission spectrum of 2-ABT4FB

$$E\,(eV) = \frac{hc}{\lambda} = \frac{1240}{\lambda} \quad (17)$$

Here, E represents energy (eV or electron volts), λ represents wavelength (nm) and ν represents wave number (cm^{-1}) that represents wavelength. Therefore, it is suggested that the 2-ABT4FB single crystal may be suitable for blue LED fabrication and visible range photoluminescence detection.

Microhardness analysis

Mechanical strength of the material was determined by the micro-hardness test. It is related to the materials mechanical characteristics, such as their yield strength and elastic constants (Berlin *et al.* 2025). For analyzing microhardness properties, SHIMADZU MHV-G21 series microhardness tester fitted with the diamond indenter is used. Hardness measurements obtained for applied loads varying from 25g-100g, with a 10s indentation constant for all cases. Using equation (18), Vickers' hardness number was determined.

$$H_v = \frac{1.8544 \times P}{d^2} \frac{kg}{mm^2} \quad (18)$$

Here, d is the average diagonal length of indentation mark (mm), H_v is Vickers hardness number (kg per mm^2) and 1.8544 is the constant of a geometrical fraction for a diamond pyramid. The variation of the hardness number with the applied load for grown 2-ABT4FB crystal is shown in Fig. 11. From the calculations, it is observed that hardness number decreases with increasing applied load which shows the normal indentation size effect. Depending on the material's binding strength, the graph exhibits either linear or nonlinear behavior. The crystal's fracture plane is mostly represented by nonlinear behavior. The size of indentation and the load are related through Meyer's law equation (19),

$P=Ad^n$ Here, A is an arbitrary constant

$$\log P = \log K + n \log d \quad (19)$$

Here, K stands for material constant, while n is Meyer index, also known as work hardening coefficient. Fig. 11 shows the plot between log P and log d. The slope indicates that the Meyer coefficient value and the graph matches a linear straight line. According to Onitsch theory, the 2-ABT4FB crystal has a soft character, as indicated by its assessed Meyer coefficient of 2 (Onitsch, 1974). The yield strength (σ_v) of the title compound can be determined using the relation as in equation 20 (Cahoon *et al.* 1971).

$$\sigma_v = \frac{H_v}{3} \quad (20)$$

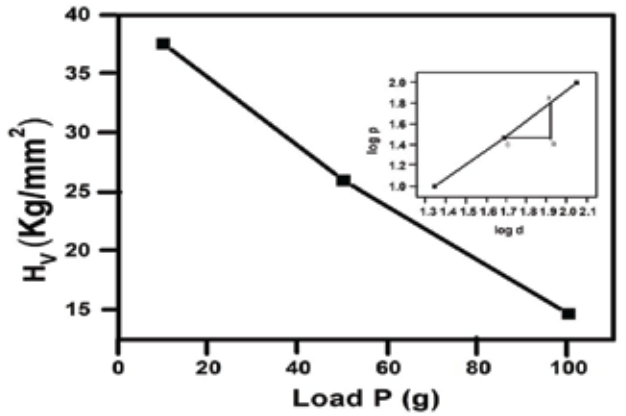

Fig. 11. Variation of Hv with load P. Plot of log d versus log P is shown in inset

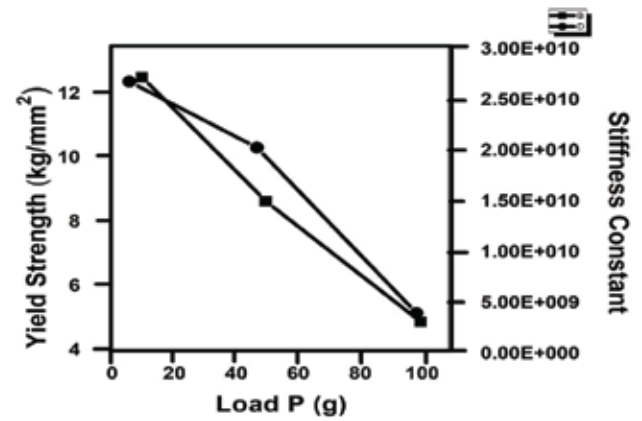

Fig. 12. Load P versus yield strength and stiffness constant

The plot of load versus yield strength is shown in Fig. 12. An elastic body's stiffness is the measure of its resistance to deformation. For varying loads, Wooster's empirical stiffness constant (C_{11}) (Wooster, 1953),

$$C_{11} = H_v^{7/4} \quad (21)$$

The grown crystals stiffness constant value increases as the applied load increases as shown in Fig. 12, represents strong binding forces within the ions in the lattice of 2-ABT4FB single crystals.

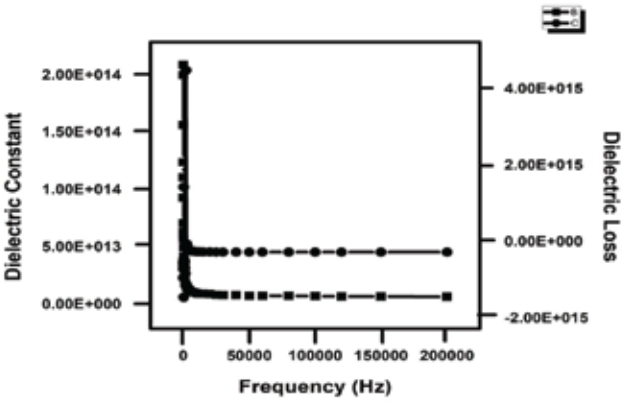

Fig. 13. Variation of dielectric constant and dielectric loss with frequency

Dielectric analysis

The dielectric examination of 2-ABT4FB single crystal was conducted utilizing Jognic's Model 2816B LCRZ Meter. The dielectric study is one of the most important analysis to study the electro-optic properties of the optical materials. Power dissipation factor could be examined through dielectric studies. Measurements of 2-ABT4FB single crystal's dielectric behavior have been made between 100 Hz and 1 MHz For the 2-ABT4FB, variations in dielectric loss and dielectric constant as functions of frequency are thought to constitute typical dielectric behavior (Baskaran *et al.* 2017). The plot of frequency versus dielectric constant and dielectric loss is shown in Fig.13. Space charge, ionic, orientation, electronic polarization are the causes of high dielectric constant at low frequencies. The very high value of dielectric constant (ε′) at low frequencies is mainly concerned due to decrease of this polarization phenomena. The low value dielectric constant (ε′) at high frequency enunciates decrease of polarizations gradually portrays lesser defects in 2-ABT4FB crystal with high optical quality thereby could meet the requirements in nonlinear optical applications (Jayaprakash *et al.* 2017). Dielectric loss of 2-ABT4FB was computed utilizing the equation (22) (Nalini *et al.* 2021),

Here, Ɛ represents the dielectric constant tan δ represents the dispersion power factor. Dissipation of energy due to the

$$\text{Ɛ}' = \text{Ɛ} \tan \delta \qquad (22)$$

ionic movement with respect to the applied filed can be quantified by studying dielectric loss (Arul *et al.* 2015). From Fig. 13 that dielectric loss decreases with respect to increase in frequency. Dielectric loss is also exhibiting the same type of variation as observed in the dielectric constant. The lower dielectric loss at high frequencies suggests that the grown crystal is having lesser defect density, which is an important phenomenon to be an active NLO material (Smyth, 1955).

Conclusion

2-ABT4FB single crystal was screened using various characterization techniques and found that the single crystal exhibits excellent optical properties. Using single-crystal XRD, the unit cell characteristics were determined, confirming the crystal position in the triclinic crystal system. The presence of the protonation was confirmed from the FTIR spectrum and the functional groups were determined. The lower cutoff wavelength and wide transparency window of the single crystal indicates the suitability of the crystal for optical device fabrication. Various optical parameters like reflectance, optical band gap energy, absorption coefficient, extinction coefficient, refractive index, urbach energy, optical conductivity, electrical conductivity, electric susceptibility and dielectric constants were calculated from the UV spectrum. The crystal exhibits blue emission at 470 nm with the band gap energy of 2.63 eV. From Vicker's microhardness study it was confirmed that the crystal belongs to soft material with the Meyer's index of 2. Single crystals dielectric behavior is analyzed and found to be high at low frequencies and decreases as the frequency increases, indicating that the crystal has good dielectric behavior.

Reference

Al-Tel TH, Al Qawasmeh RA and Zaarour R (2011), Design, synthesis and in vitro antimicrobial evaluation of novel Imidazo[1,2-a]pytidine and imidazole[2,1-b][1,3] benzothiazole motifs, *Eur. J. Med. Chem.* **46:** 1874-1881. https:// doi.org/ 10.1016/ j.ejmech.2011.02.051.

Anis M, Shkir M, Baig MI, Ramteke SP, Muley GG, Alfaify S, Ghramh HA (2018), Experimental and computational studies of L-tartaric acid single crystal grown at optimized pH, *J. Mol. Struct.* **1170:** 151–159. https://-doi.org/10.1016/j.molstruc.2018.05.073.

Anis M and Muley GG (2016), Single crystal growth and enhancing effect of glycine on characteristic properties of bis thiourea zinc acetate crystal, *Phys. Scr.* **91:** 85801-85808. https://doi.org/ 10.1088/ 0031-8949/91/ 8/085801.

Asep Bayu Dani Nandiyanto, Rosi Oktiani and Risti Ragadhita (2019), How to read and interpret FTIR spectroscope of organic material, *Indo. J. Sci. Tech.* **4:** 97-11. 8https://doi.org/10.17509/ijost.v4i1.15806.

Arul H, Rajan Babu D, Ezhil Vizhi R and Bhagavannarayana G (2015), Investigation on nucleation on kinetics, structural and dielectric properties of an organic NLO single-crystal I-Histidinium maleate, *J. Cryst. Growth.* **423:** 22-27. https://doi.org/10.1016/j.jcrysgro.2015.04.021.

Baskaran P, Vimalan M, Anandan P, Bakiyaraj G, Kirubavathi K and Selvaraju K (2017), Synthesis, growth and characterization of a nonlinear optical crystal: L-Leucinium perchlorate, *J. Tai. Uni. Sci. J.* **11:** 11-17. https://doi.org/10.1016/j.jtusci.2016.03.003.

Berlin Beno TL, Maria Lenin M and Abina Shiny RS (2025), Synthesis and characterization of semi-organic sodium thiocyanate potassium sulphate (STPS) crystal using slow evaporation method, *Ind. J. Pu. App. Phy.* **63:** 240-254. https://doi.org/10.56042/ijpap.v63i3.15628.

Braga D (2007), Making Crystals by Design: Methods, Techniques and Applications. 1st Ed. (Wiley-VCH, Euro), pp 241.

Brain SF, Antony JH, Peter WG, Smith and R Austin and Tatchell (1989), Vogel's Text Book of Practical Organic Chemistry. 5th Ed. (Longman Scientific & Technical, New York), pp 256.

Cahoon JP, Broughton WH and Katzuk AR (1971), The determination of yield strength from hardness measurement, *Metall. Mat. Trans.* **2:** 1979-1983. https://doi.org/10.1007/BF02913433.

Denys Cook (1964), Protonation site in organic bases from infrared x-h deformation modes, *Cana. J. Chem.* **42:** 2292. https://doi.org/10.1139/v64-336

Dhanaraj PV, Sudan T and Rajesh NP (2010), Growth, spectral and optical characterization of a novel nonlinear optical organic material: D-Alanine DL-Mandelic acid single crystal, *Curr. Appl. Phys.* **10:** 1349-1353. https://doi.org/10.1016/j.cap.2010.04.008

Frizon TEA, Salla CAM, Grillo F, Rodembusch FS, Camara VS, Silva Jr HC, Zapp E, Junca Ed, Galetto F.Z, De

Costa AM, Pedroso GJ, Chepliki A, Saba S and Rafique J (2023), ESIPT-based benzazole-pyromellitic diimide derivatives. A thermal, electrochemical and photochemical investigation, *Mole. Bio. Spec.* **288:** 122050. https://doi.org/10.1016/j.saa.2022.122050.

HalilIlkimen, YaseminTekşen, CengizYenikaya, IremTurhan, TuncayTunç and Musa Sari (2018), Synthesis, characterization and pharmacological evaluation of the proton transfer salts of 2-aminobenzothiazole derivatives with 5-sulfosalicylic acid and their Cu(II) complexes, *J. Coordi. Chem.* **71:** 1-12. https://-doi.org/10.1080/00958972.2018.1504035.

Hari Singh Nalwa (2001), Handbook of surfaces and Interfaces of materials. 1st Ed. (Academic press, Japan): p 71.

Hassel (1970), Structural Aspects of Interatomic Charge-Transfer Bonding, *O. Science,* **170:** 497-502.https://doi.org/ 10.1126/science. 170.3957.497.

Hiral Raval B, Parekh B, Parikh KD and Joshi MJ (2019), Growth and Characterizations of Organic NLO Imidazolium L-Tartrate (IMLT) Single Crystal, *Hin. Adv. Con. Mat. Physics.* p 3853215. https://-doi.org/10.1155/2019/3853215.

İlkimen H, Yenikaya C, Sarı M, Bülbül M, Tunca E and Dal H (2014), Synthesis and characterization of a proton transfer salt between 2,6-pyridinedicarboxylic acid and 2-aminobenzothiazole, and its complexes and their inhibition studies on carbonic anhydrase isoenzymes, *J. Enzyme. Inhib. Med. Chem.* **29:** 353-361.https://-doi.org/10.3109/14756366.2013.782299.

Jayaprakash P, Peer Mohamed M and Lydia Caroline M (2017), Growth, spectral and optical characterization of a novel nonlinear optical organic material: D-Alanine DL-Mandelic acid single crystal, *J. Mol. Struct.* **1134:** 67-77. https:// doi.org/ 10.1016/ j.molstruc. 2016.12.026.

Jin S, Yan P, Wang D, Xu Y, Jiang Y and Hu L (2012), Salt and co-crystal formation from 6-bromobenzo[d]thiazol- 2-amine and different carboxylic acid derivatives, *J. Mol. Struct.* **1016:** 55–63. https://doi.org/ 10.1016/j.molstruc.2012.02.036.

Kamal A, Srikanth Y.V.V, NaseerAhmed Khan M, Ashraf M, Kashi Reddy M, Sultana F, Kaur T, Chashoo G, Suri N, Sehar I, Wani ZA and Saxena SK (2011), 2-Anilononicotinyl linked2-aminobenzothiazoles and [1,2,4]triazolo[1,5-b][1,2,4] benzothiadiazine conjugates as potential mitochondrial apoptotic inducers, *Bio. Med. Chem.* **19:** 7136-7150. https://doi.org/ 10.1016/ j.bmc. 2011.09.060.

Karuppasamy K, Kamalesh T, Anitha, Muthu Senthil Pandian K, Ramasamy P and Sunil Verma (2020), Design and growth of novel organic molecular quinolone 4-nitrophenol (QNP) single crystals: For nonlinear optical (NLO) applications, *J. Mol. Struct.* **1210:** 1 11.https://doi.org/10.1016/j.molstruc.2020.128036.

Kochuparampil AP, Joshi JH and Joshi MJ (2017), Growth, structural, spectroscopic, thermal, dielectric and optical study of cobalt sulphide-doped ADP crystals, *Mod. Phy.B.* **27:** 1-21. https://doi.org/ 10.1142/ S0217984917502463.

Kornelia Kowalska and Damian Trzybinskiand Artur Sikorski (2015), Influence of the halogen substituent on the formation of halogen and hydrogen bonding in co-crystals formed from acridine and benzoic acids, *Cryst. Eng. Comm.* **37:** 1-14. https://doi.org/ 10.1039/ C5CE01321F.

Lee SH, Jabinsek M, Hauri CP and Kwon OP (2016), Solid-state photochemistry, *Cryst. Eng. Comm.* **18:** 7180-7185. https://doi.org/10.1039/C6CE90146H.

Li Li, Xiaoqi Zhao, Ning Xiao, Yongjie Wang, Zhiliang Wang, Shuguang Yang and Xianju Zhou (2015), Synthesis, structure and fluorescence studies of the lanthanide complexes with 4-fluorobenzoic acid, Ino. Chi. Act. 426: 107-112.https://doi.org/10.1016/j.ica.2014.11.035.

Mahalakshmi N and Parthasarathy M (2024), Photoluminescence, scanning electron microscope and atomic force microscope analyses of organic NLO single crystal of hippuric acid for opto-electronic and photonic applications, J. Sci. Res. 16: 449-457.https://doi.org/10.3329/-jsr.v16i2.67430.

Mahendra K, Brian Jeevan Fernandes, JayadevPattar, Swati Pujar, Nagaraja BS, Ramesh KP and Udayashankarc NK (2023), Systematic investigation and comparison of oxalic acid dehydrate, ammonium oxalate hydrate and ammonium hydrogen oxalate oxalic acid dehydrate single crystals, Mater Sci and Eng B. 288: 116157.https://doi.org/10.1016/j.mseb.2022.116157.

Mark Fox (2013), Optical Properties of Solids. 2nd Ed. (OxafordUniversity Press, New York), pp 113.

Murugan T and Murugesan KS and Boaz BM (2022), Growth, linear and nonlinear optical property and dielectric studies of an efficient organic ionic single crystal: 2-amino-5-methyl-pyridinium trifluoroacetate for optoelectronic devices, *Ind. J. Phy.* **96:** 3797. https://doi.org/10.1007/s12648-022-02335-x.

Nalini H, Thairiyaraja M, Arunagiri C, Manivannan D, Charles Vincent V, Kirubavathi K and Selvaraju K (2021), Crystal growth, structural, nonlinear, optical and theoretical investigations of L-histidiniumtrichloroacetate single crystals, *Bull. Mater. Sci.* **44:** 1-17. https://doi.org/10.1007/s12034-020-02319-9.

Omer BahadirMergen, ErtanArda, Selim Kara and Onder-Pekcan (2018), Effects of GNP addition on optical properties and band gap energies of PMMA films, Wiley Online Librar. **5:** 1862-1869. https://doi.org/10.1002/pc.24948.

Onitsh EM (1974), Uber die Mikroharte der Metalle (Mikroskopie. 1st Ed., p 6.

Prabukanthan P, Raveendiran C, Harichandran G and PerumalSeenuvasakumaran (2020), Synthesis, crystal growth, crystal structure, optical, thermal, biological and NLO studies of heterocyclic compound N-(1,3-benzothiazol-2-yl)-2-methoxybenzamide, *Res. Chem.* **2:** 100083. https://doi.org/10.1016/j.rechem.2020.100083.

Ramin Javahershenas, Jianlin Han, Mosstafa Kazemi and Pater JJ (2024), Recent advances in the application of 2-aminobenzothiazole to the multicomponent synthesis of heterocycles, *Chemistry Open.* **13:** 1.https://-doi.org/10.1002/open.202400185.

Sadat ME, Baghbador MK, Dunn AW, Wagner H, Eding RC, Zhang J, Xu H, Pauletti GM, Mast DB and Shi D (2014), Photoluminescence and photothermal effect of Fe3O4 nanoparticles for medical imaging and therapy, App. *Phys. Lett.* **105:** 091903.https://-doi.org/10.1063/1.4895133.

Sangeetha T, Gayathri K, Krishnan P, Sivakumar N, Kanagathara N and Anbalagan G (2014), Growth, optical, thermal, dielectric and microhardness characterizations of melaminiumbis (trifluoroacetate) trihydrate single crystal, *J. Cryst. Growth* **389:** 30-38. https://-doi.org/10.1016/j.jcrysgro.2013.11.026.

Sharma V, Kaur G, Singh A, Banerjee B and Gupta VK (2020), Synthesis and Characterization of 2 Amino-benzothiazol and 1-Methylisatin Co-Crystal, *Crystallogr. Rep.* **65:** 1195. https://doi.org/ 10.1134/S1063774520070172.

Shubashini I and Jebas SR (2025), Growth, spectral, electrical, photoluminescence, thermal, mechanical and dielectric Studies of 2-hydroxy benzoic acid (Metabolite of Drug Aspirin) single crystal, *J. Sci. Res.* **17:** 211-225. https://doi.org/10.3329/jsr.v17i1.74784.

Smyth GP (1955), DielectricBehaviour and Structure (McGraw-Hill, New York), pp 838.book

Tariq Mustafa, Bindu Raina, Harjinder Singh, Yaseen Ahmad and K KBamzai (2023), Crystal growth, structure, morphology, optical, thermal and electrical studies of dysprosium chloride-thiourea semi-organic complex crystal, Pramana. *J. Phys.* **139:** 1-13.https://doi.org/10.1007/s12043-023-02615-z.

Tauc J (1974), Amorpous and liquid semiconductors. 1st Ed. (Plenum press, New York), pp 159.

Urbach F (1953), The long-wavelength edge of photographic sensitivity and of the electronic absorption of solids, *Phys. Rev.* **92:** 1324.https://doi.org/10.1103/PhysRev.92.1324.

Vijayalakshmi G, Perianayagi L, Jebasingh Kores J, Ravindran Durai Navaagam B and Ilavarasi JJ (2025), Unveiling the anticancer potential: Exploring 4-fluorobenzoic acid and piperazine through spectroscopic, X-ray diffraction, DFT and molecular docking analysis, *J. Mol. Str.* **1322:** 140507.https://-doi.org/10.2139/ssrn.4902932.

Wooster WA (1953), Physical Properties and Atomic Arrangements in Crystals. 1st Ed. (University of Cambridge, England), pp 344.

Yakuphanoglu F, Sekerci M and Ozturk O F (2004), The determination of the optical constants of Cu(II) compound having 1-chloro-2,3-o-cyclohexylidinepropane thin film, *Opt. Commun.* **239:** 275-280. https://-doi.org/10.1016/j.optcom.2004.05.038.

Yongbin Hua, Weiguang Ran and Jae Su Yu (2021), Excellent photoluminescence and cathodoluminescence properties in Eu3+-activated Sr2LaNbO6 materials for multifunctional applications, *Chem. Eng. J.* **406:** 127154. https://doi.org/10.1016/j.cej.2020.127154.